Different hue coding underlying figure segregation and region detection tasks

Takehiro Nagai

Department of Psychology,
University of California, San Diego, CA, USA

Keiji Uchikawa

Department of Information Processing,
Tokyo Institute of Technology, Yokohama, Japan

Figure segregation from its background is one of the important functions of color vision for our visual system because it is a preliminary to shape recognition. However, little is known about the chromatic mechanisms underlying figure segregation as opposed to those underlying mere color discrimination and detection. We investigated whether there are differences in color difference thresholds between a shape discrimination task (involving figure segregation) and a simple region detection task. In the shape discrimination task the observer discriminated the shapes of two figures, which could be segregated from their background on the basis of a color direction (hue) difference. In the region detection task the observer simply detected a square region against its background. Thresholds of color direction differences from a range of background color directions were measured for each task. In addition, we added saturation variation in one condition to investigate the involvement of the cone-opponent channels in those tasks. First, the results showed that the saturation variation increased the thresholds evenly for all background color directions. This suggests that higher-order color mechanisms rather than the early cone-opponent mechanisms are involved in both of the two tasks. Second, the shapes of the background color direction-threshold functions were different between the two tasks and these shape differences were consistent across all observers. This finding suggests that hue information may be encoded differently for shape discrimination and region detection. Furthermore, differences in spatial frequency components and in the requirement for orientation extraction rarely affected the shapes of the threshold functions in additional experiments, suggesting the possibility that hue encoding for shape discrimination differs from encoding for region detection at a late stage of form processing where local orientation signals are globally integrated.

Keywords: color, figure-ground segregation, form vision, cone-opponent mechanism, psychophysics

Citation: Nagai, T., & Uchikawa, K. (2009). Different hue coding underlying figure segregation and region detection tasks. *Journal of Vision, 9*(9):14, 1–19, http://journalofvision.org/9/9/14/, doi:10.1167/9.9.14.

Introduction

The ability to detect or discriminate color is an important ability, as it allows us to detect an object based on the color difference between it and its background. For example, monkeys can easily detect reddish fruits from a greenish bush using color differences, even when the luminance information is quite noisy (Mollon, 1989).

There are a variety of studies examining the chromatic properties of mechanisms underlying color discrimination and detection (Stabell & Stabell, 1984; Wright & Pitt, 1934). One of the important findings about color detection and discrimination is the existence of cone-opponent mechanisms (Boynton, 1979; Krauskopf, Williams, & Heeley, 1982). It has been demonstrated, for example, that a variety of chromatic discrimination thresholds such as the MacAdam ellipse (MacAdam, 1942) can be explained by means of the three mechanisms: Luminance, L-M, and S mechanisms (Boynton & Kambe, 1980; Boynton, Nagy, & Olson, 1983).

In addition, some recent studies indicated that there are higher-order chromatic mechanisms tuned to different directions in a color space other than the cardinal directions (Krauskopf et al., 1982) that correspond to the responses of the three cone-opponent mechanisms identified physiologically in the lateral geniculate nucleus (Derrington, Krauskopf, & Lennie, 1984). For example, in detection of a Gabor patch (Gegenfurtner & Kiper, 1992) and in texture discrimination (Li & Lennie, 1997), noise along directions intermediate between the cardinal directions raises the thresholds only along the same direction but not along the orthogonal directions. These results cannot be explained only by independent effects of the cone-opponent mechanisms. Some simple color discrimination experiments similarly suggest the existence of such higher-order chromatic mechanisms (Krauskopf & Gegenfurtner, 1992; Sankeralli & Mullen, 1999). They measured color discrimination threshold contours around a reference color, which was offset from the color to which the observer was adapted in the cone-opponent space. In their results, the thresholds formed an ellipse whose major axis is along the line from the adaptation

doi: 10.1167/9.9.14 Received October 26, 2008; published August 28, 2009 ISSN 1534-7362

color to the reference color. These results cannot be explained only by the cone-opponent mechanisms. These experiments have helped to clarify the chromatic properties of the mechanisms contributing to color discrimination and detection.

In addition to mere discrimination and detection, segregation of a figure from its background is another important function of color vision as Mollon (1989) has stated, because it is a preliminary to shape recognition. In the past, form vision was generally thought to be mainly mediated by luminance information (Livingstone & Hubel, 1987). However, Mullen, Beaudot, and MacIlhagga (2000) showed that global contour integration from multiple Gabor patches was comparably good for both luminance and color vision. Moreover, Mullen and Beaudot (2002) indicated that discrimination of two shapes defined by isoluminant edges, as well as shapes defined by luminance edges, could be performed at a hyperacuity level of resolution. These results support the role of color vision in form perception. However, there have been only a few studies investigating the chromatic properties of mechanisms underlying chromatic form perception (Cardinal & Kiper, 2003; Mandelli & Kiper, 2005; Wilson & Switkes, 2005), and those properties still remain unclear.

One central question is whether there are any differences between the chromatic mechanisms underlying simple discrimination and form perception. In form perception, at least two processes are necessary in addition to those involved in discrimination or detection. One is extraction of local orientation at the contour of a form, and the other is global integration of local orientations to create a form (Wilkinson, Wilson, & Habak, 1998; Wilson & Wilkinson, 1998). Accordingly, it would not be surprising if form perception based upon chromatic information may involve chromatic mechanisms different from those involved in discrimination. Though Nagai and Uchikawa (2008) suggested that the thresholds for figure segregation, a task relevant to form vision, may behave on the cone-opponent plane as color discrimination thresholds do, they did not measure color discrimination thresholds and did not directly compare the thresholds between those different tasks. Thus it has not been clarified whether different mechanisms with different chromatic properties are involved in form perception and simple discrimination.

In the current study, we demonstrate the possibility that the mechanisms involved in simple discrimination and form perception have different chromatic properties. We conduct two kinds of tasks using similar sets of colored texture stimuli. One is shape discrimination, a task involving form perception, in which the observer segregates two figures from their background using chromatic differences and compares the shapes of the two figures. The other is region detection, a discrimination task, in which the observer merely detects the square region against its background on the basis of a chromatic difference. The thresholds for the two tasks are measured separately and then compared. At the same time, we use a spatial random noise similar to that used in the previous studies employing texture stimuli (Hansen & Gegenfurtner, 2006; Li & Lennie, 1997) to examine whether the cone-opponent mechanisms can explain the shape discrimination thresholds and region detection thresholds.

Experiment 1—Shape discrimination

To compare chromatic characteristics of mechanisms involved in the shape discrimination and region detection tasks, we measured thresholds for the shape discrimination task in Experiment 1, and for the region detection task in Experiment 2.

Methods

Apparatus

The stimulus was presented on a CRT monitor (Nanao T766, 75 Hz), which was carefully calibrated with Topcon SR-2. Cambridge Research System Bits++ enabled us to use 14 bit levels for each of the RGB guns. A PowerMac G4 (450 MHz) controlled the experimental procedures. The observer binocularly viewed the stimulus 57 cm away from the screen.

Preliminary experiment

The colors of the stimulus were defined in the DKL space (Derrington et al., 1984; MacLeod & Boynton, 1979) based on the cone fundamentals of Smith and Pokorny (1975) in all experiments in this paper. Because the scales of the axes of the DKL space (Luminance, L-M, and S) were arbitrary, we measured detection thresholds from the origin (equal energy white of 20 cd/m^2) in both of the negative and positive directions on each of the three axes in a preliminary experiment for each observer. These thresholds can be conceived of as indices to approximately equate visibility for different axes and directions.

In the preliminary experiment, the stimulus was a uniform square (its size and position were identical to stimuli of Experiment 2 in this study. See Experiment 2 for details) to the right or left of a black fixation cross on a uniform gray full-screen background of equal energy white of 20 cd/m^2 (the origin of the DKL space). The observer responded if the square was in the left or right after the stimulus presentation. We adopted the mean of these measured thresholds in the negative and positive directions as a unit distance on each axis for each observer

to define intermediate directions between the cardinal directions.

We initially defined saturation a in this space as a distance from the origin to a color in the isoluminant plane. But we found in the preliminary experiment that the detection thresholds measured were different between the positive and negative directions even on the same axis. We wanted to measure thresholds of color direction differences for the two tasks in the main experiments, but (subjective) saturation differences between color directions were expected to influence those thresholds (because larger saturation leads to larger color differences even for identical color direction differences). Therefore, to compensate the effect of those saturation differences, an adjusted saturation a' for each of different color directions was defined according to

$$a' = a/\sqrt{(l_1\cos\theta_a)^2 + (s_1\sin\theta_a)^2} \qquad 0 \le \theta_a < \frac{1}{2}\pi, \qquad (1)$$

$$a' = a/\sqrt{(l_2\cos\theta_a)^2 + (s_1\sin\theta_a)^2} \qquad \frac{1}{2}\pi \le \theta_a < \pi, \qquad (2)$$

$$a' = a/\sqrt{(l_2\cos\theta_a)^2 + (s_2\sin\theta_a)^2} \qquad \pi \le \theta_a < \frac{3}{2}\pi, \qquad (3)$$

$$a' = a/\sqrt{(l_1\cos\theta_a)^2 + (s_2\sin\theta_a)^2} \qquad \frac{3}{2}\pi \le \theta_a < 2\pi, \qquad (4)$$

where a is saturation defined as described above, θ_a is a color direction, l_1 and l_2 are the thresholds for the positive and negative directions along the L-M axis divided by the average between them, and s_1 and s_2 are those along S axis. This manipulation changes saturation of a color based on the thresholds and color directions measured in the preliminary experiment (e.g., for identical a' values on the L-M axis the a values for positive and negative directions should be proportional to the preliminary thresholds). We will use a' instead of a to represent saturation in our experiments.

The stimulus used in Experiment 1 is shown in Figure 1a. It is a multi-colored texture composed of 83 × 50 elements on a gray background (equal energy white of 20 cd/m^2, the origin of the DKL space we used). The size of the texture was 17 deg × 27 deg, the size of each element was about 0.26 × 0.26 deg, and the width of the gray gap between adjacent elements was 3.9 min. Figure 1b shows how we constructed the elements in the texture. Each element was an octagon whose vertices were made by

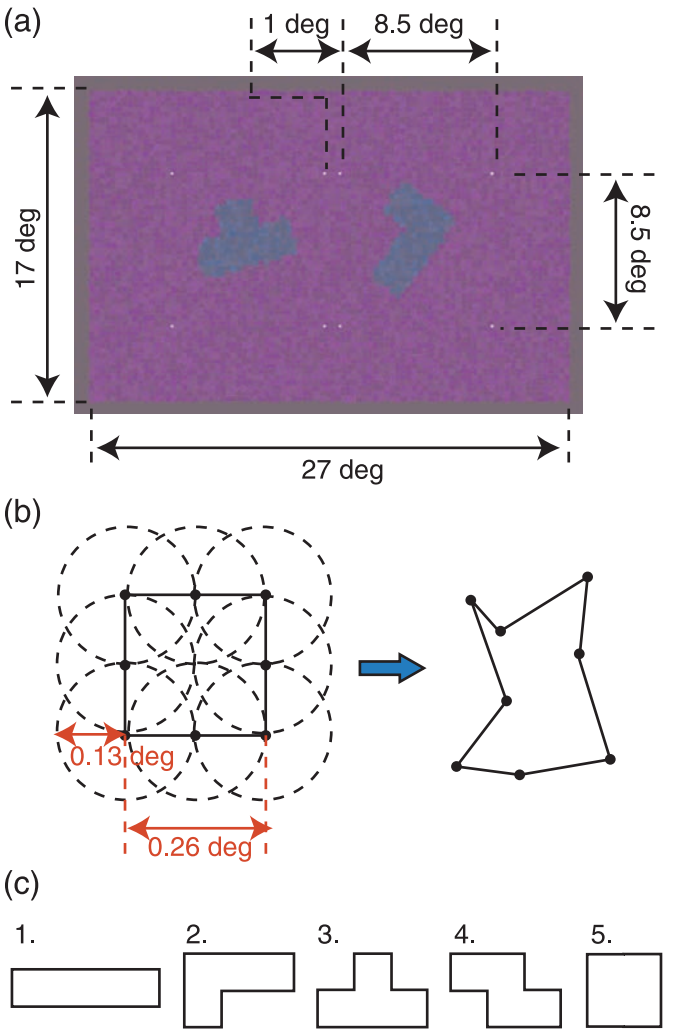

Figure 1. (a) Stimulus texture. The green regions are called the test regions, and the purple regions the background region. (b) Scheme of how each texture element was shaped. (c) Shapes of the test regions.

moving 4 vertices and 4 midpoints of a 0.26 deg × 0.26 deg square within circles whose centers were at the original positions and radii were 0.13 deg. These 8 points formed the vertices of the octagonal element; to define a single closed region, the vertices were connected in the order of their direction from the center of the original square. Three vertices were shared with each of the adjacent elements. This texture was divided into two kinds of regions: two test regions and a background region. The two test regions were at the random positions within the 8.5 deg × 8.5 deg squares, respectively, each of which was created by four white dots shown in Figure 1a (these dots were visible also in the experiments) and which were separated by 1 deg. The shapes of the test regions are shown in Figure 1c. They were constructed by connecting 4 squares each of size 1.6 deg × 1.6 deg. Their shapes were similar to the

blocks used in the video game Tetris (http://en.wikipedia.org/wiki/Tetris). The area of the test region could not be a cue for the observer's responses in judging shape differences because the areas of all the shapes were equal. In addition, the shapes were randomly rotated, preventing the observer from responding based on orientation similarity. The shapes of the two test regions in a stimulus were either identical or different. When they were different, one of the 4 neighboring pairs in Figure 1c was selected as the pair of the test region shapes (e.g. 1 and 2, 2 and 3, 3 and 4, or 4 and 5 in Figure 1c). The background region was the region of the texture outside of the two test regions.

The colors of the elements included in the test regions and background region were uniformly selected from different color distributions in the DKL space. Therefore, the observer could segregate the test regions from the background region using the color distribution difference. Figure 2 illustrates the color distributions of the test and background regions in the isoluminant plane of the DKL space. They were on lines from the origin in the isoluminant plane. Therefore their hue can be roughly represented by the color directions; we defined the positive direction along the L-M axis as 0 deg, and that along the S axis as 90 deg. The distributions of the test and background regions were different only in their color directions, while their saturation distributions were identical in a given condition. In addition, random luminance variation from a uniform distribution ranging from −7.5 to 7.5 threshold units was also added to both the distributions to suppress effects of luminance mechanisms.

Sixteen color directions were used as the directions of the background color distributions (θ in Figure 2): from 0 to 337.5 deg in 22.5 deg steps. Color directions rotated counterclockwise from each background color distribution ($\theta + d\theta$ in Figure 2) were used as the test color distributions.

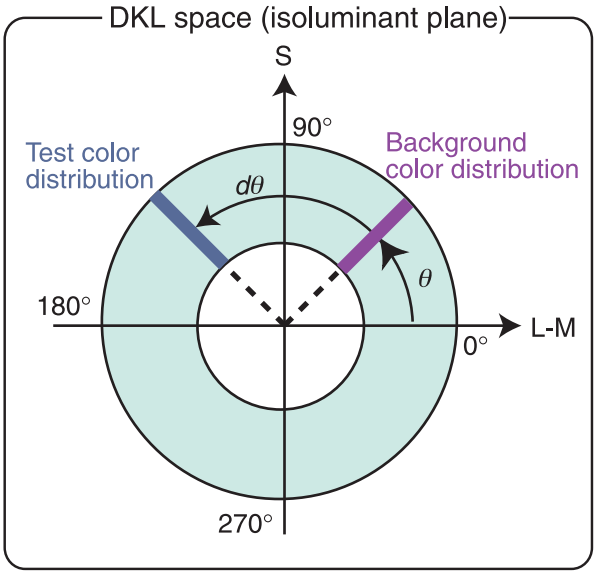

Figure 2. Diagram of the color distributions of the test and background regions in the isoluminant plane of the DKL space used.

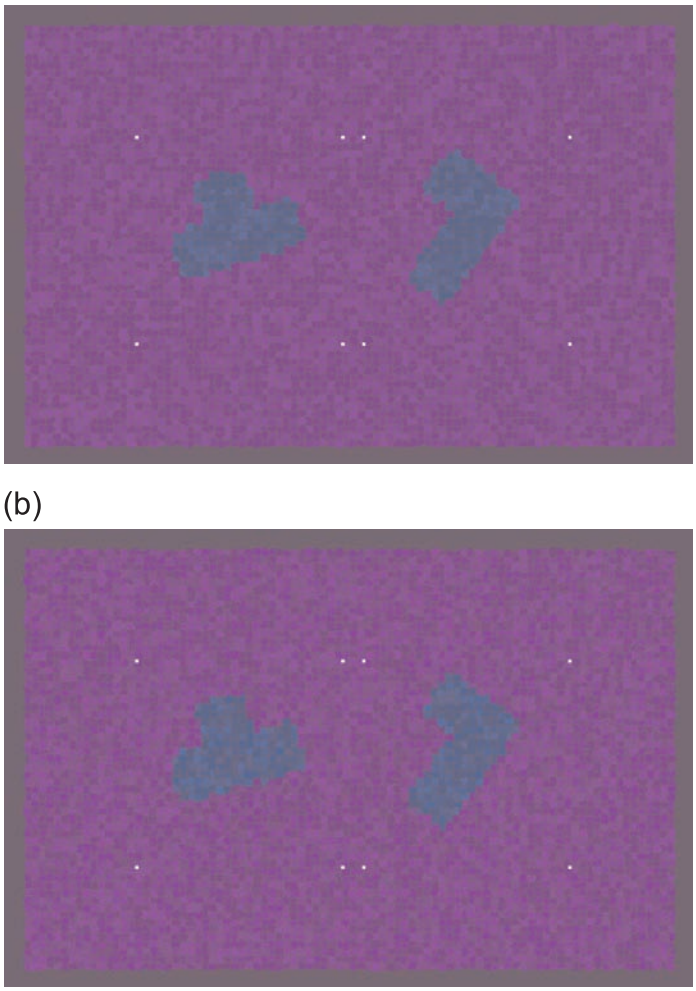

Figure 3. Stimuli for (a) multiple-saturation condition and (b) single-saturation condition at the mean saturation from (a). The perceived difference in stimulus appearance for these different saturation conditions is quite small (as corroborated by our actual experiments).

We had two kinds of saturation distributions: the multiple-saturation condition and the single-saturation condition. Stimuli for those two conditions are shown in Figure 3. In the multiple-saturation condition, the color distributions had a uniform saturation variation ranging from 15 to 30 (i.e., the saturations varied from element to element in a texture). In contrast, the color distributions of the single-saturation condition had no saturation variations (i.e., the saturations of all elements were the same in a stimulus). The single-saturation condition included several conditions in which different saturations were used; the saturations for the observer TN were 15, 18.75, 22.5, 26.25, and 30, and those for the other observers were 15 and 30. We introduced those saturation conditions with

the expectation that they could help to clarify whether the cone-opponent channels and mechanisms that completely distinguish between hue and saturation could be involved in performing those tasks (see Results for further explanation on our rationale).

Procedure

The observer adapted to the gray background for 3 minutes before each session. At the beginning of each trial, a black fixation point was presented at the center of the screen on a full-screen gray background. Then, the stimulus was presented after the observer was ready and pressed a key. Two texture stimuli were successively presented for 247 ms each separated by the gray background presentation for 1000 ms. In one of those two stimuli the two test regions were of different shapes, and in the other stimulus they were of an identical shape. The shapes were independently chosen for the first and second stimuli. After the stimulus presentation the observer indicated which of the two stimuli had different test shapes, a two alternative forced choice (2AFC) procedure. Beeps informed the observer whether his response was correct or incorrect.

In each session, one of the saturation distribution conditions and all of the 16 background color directions were tested. The 1-down 2-up staircase method adjusted the difference in color directions between the test and background color distributions ($d\theta$ in Figure 2). The number of steps of the test distribution directions was 9 for each background color direction, and the step sizes were different between the observers and experimental conditions to increase efficiency of threshold estimation, because thresholds depended on the observers and experimental conditions. Those step widths were fixed among sessions within each observer and condition. A session had an upward staircase (starting from no color difference) and a downward staircase (starting from a maximum color difference) for each condition. Both staircases measured sensitivities in the counterclockwise direction in the isoluminant plane. Each staircase finished after six reversals. The number of trials included in a session was approximately 720. The observer conducted 5 sessions for each saturation condition.

Observer

One of the authors (TN) and two naïve observers (TF and SN) participated in Experiment 1. All of them had normal or corrected-to-normal acuity. The Farnsworth 100 hue test and the Ishihara color blindness plates confirmed that all of them had normal color vision.

Analysis

We could derive from the raw data the probability of correct response as a function of the color direction difference between the test and background color distributions for each condition. The threshold was defined as the difference in color direction that corresponded to 75% correct responses by fitting a logistic function with the maximum likelihood method.

Results

Thresholds

The thresholds measured in Experiment 1 are shown in Figure 4. In addition, these thresholds are also shown in Figure 5 in the form of polar plots to help intuitively see these function shapes. The thresholds varied with background color direction in each saturation condition for all observers ($p < 0.001$ for every individual observer according to a chi-squared test). The threshold trends seemed similar for different saturation conditions within each observer, but appeared different across observers. In addition, when the thresholds for different saturations (for the single-saturation conditions) were compared, the thresholds tended to decrease as the saturation increased (the main effect of the saturation was significant; $p < 0.001$ for every individual observer). These results indicate that the color direction difference thresholds for the shape discrimination task cannot be equal even in the cone-opponent plane normalized by each individual observer's detection thresholds. Detection thresholds were greater at the lower saturations.

In the multiple-saturation condition the mean stimulus saturation was 22.5. But for observer TN's, the thresholds in this condition were higher than the thresholds for single-saturation condition with saturation of 22.5, and lay between those of the single-saturation conditions with saturations of 15 and 18.75. For other observers, the thresholds of the multiple-saturation condition were closer to those for saturation of 15 than 30. This suggests that saturation variation raised the thresholds to some extent.

To see the effects of the stimulus saturation in more detail, the thresholds for the single saturation condition averaged across the background color directions are shown in Figure 6. First, the thresholds in the color direction decrease with the stimulus saturation. This suggests that hue and saturation are not independently processed in the visual system when comparing two shapes using hue differences. Second, the threshold for the multiple-saturation condition seems high in comparison with the overall threshold levels for the single-saturation condition as described above. Finally, the thresholds in the Euclidian distance also depend on the saturation; they increase with the saturation.

Effects of saturation variation

As noted above, we included two saturation distribution conditions: multiple-saturation condition and single-

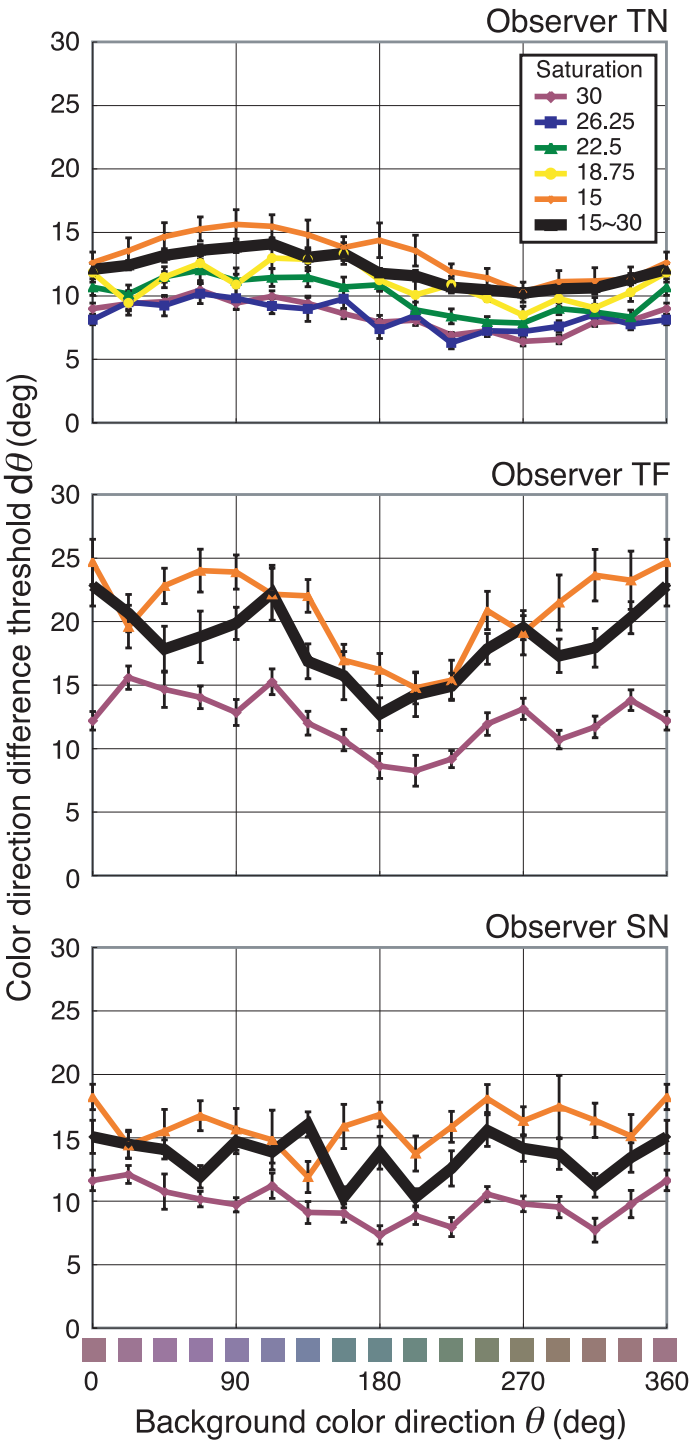

Figure 4. Shape discrimination thresholds measured in Experiment 1. The background color direction is shown on the horizontal axis, and the threshold is shown on the vertical axis. The colored lines represent the results for the single-saturation conditions with different saturations, and the black lines represent the results for the multiple-saturation condition. The error bars are the standard errors derived from the maximum likelihood method. Each panel corresponds to one observer's results.

saturation condition. By comparing the results for these two conditions, we expected to clarify two issues: 1) whether only independent cone-opponent channels are responsible for determining thresholds, and 2) whether only mechanisms that completely distinguish between hue and saturation (i.e., independent mechanisms that process those two features respectively) are responsible for determining thresholds.

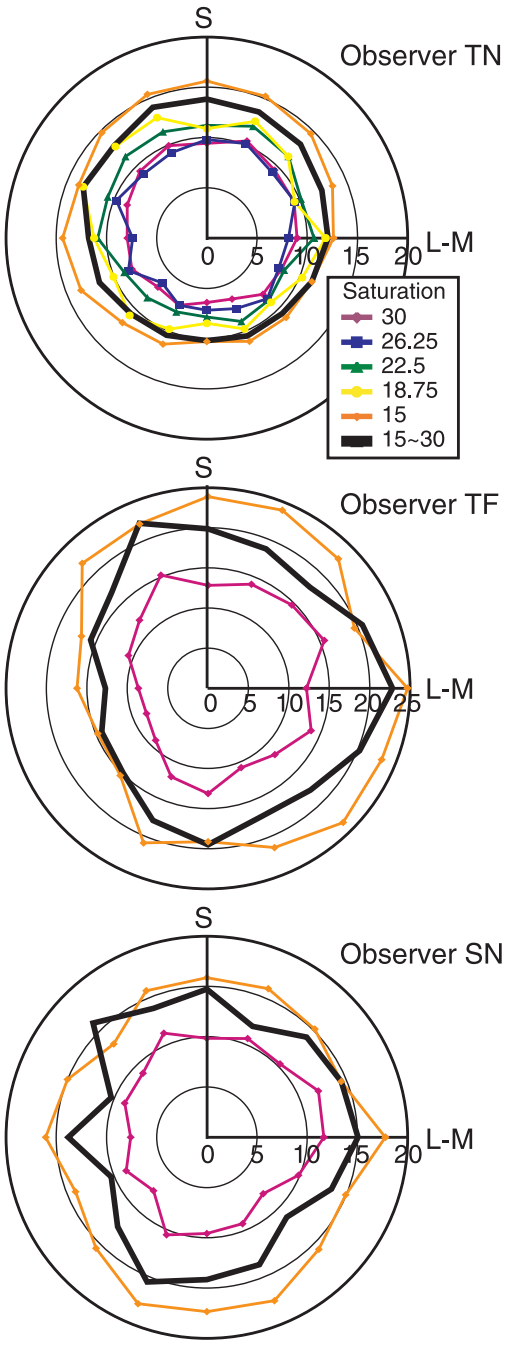

Figure 5. The same thresholds as Figure 4 in the form of polar plots. L-M coordinates are shown on the horizontal axis and S on the vertical axis. The colors of the plots correspond to saturation conditions. Each graph corresponds to each observer's results.

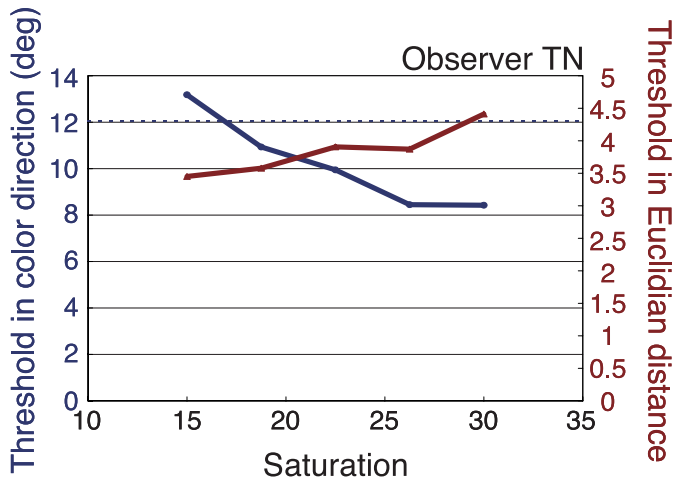

Figure 6. Thresholds for the single-saturation condition in Experiment 1 averaged across the background color directions as a function of saturation. The blue solid line represents the thresholds expressed as color direction differences (the same as those in Figure 4), and the brown line represents the thresholds expressed as Euclidian distances in the isoluminant plane. The blue dotted line is the threshold for the multiple saturation condition. Threshold in the color direction difference is shown on the left vertical axis, and that in the Euclidian distance on the right axis.

We now consider the expected effects of saturation variation on shape discrimination thresholds in two extreme cases: one where shape discrimination relies only on the responses of the cone-opponent channels, and the other where it relies only on chromatic mechanisms that completely distinguish between hue and saturation. These expectations are shown in Figure 7. Consider the first case where shape discrimination is based only on the cone-opponent channels' responses (Figure 7a). When the background color direction is one of the cardinal directions, the shape discrimination should rely on the response of the other channel because the test color distribution was different from the background color distribution only in color direction; for example, the visual system should rely on the response of the L-M channel if the background color direction was 90 deg. In this case, the saturation variation should not affect shape discrimination performance, since the channel responsible for the task and that affected by the saturation variation were different. In contrast, when the background color direction is an intermediate one such as 45 deg, the visual system should rely on responses of both of the cone-opponent channels. In this case, the saturation variation will act as random noise that limits shape discrimination performance, because the task will depend on signals from both channels and the saturation variation will create variation in both signals. Thus we expect the saturation variation effects shown in Figure 7a in this case. On the other hand, if the shape discrimination task relied only on responses of chromatic mechanisms that completely distinguish saturation and hue, saturation variation could not affect shape discrimination performance at all (Figure 7b) because the task was conducted based on hue differences in this case.

To derive the effects of saturation variation from our results, we divided the thresholds for the multiple-saturation condition by the mean of the thresholds for the single-saturation conditions in each background color direction. We refer to this value as Saturation Variation Effect (SVE). The SVEs as functions of the background color direction for all observers are shown in Figure 8a. Neither of the predictions of Figure 7 is upheld. The SVEs were more than 1 for almost all color directions and all observers, indicating that the saturation variation acted as a source of noise that disrupted shape discrimination

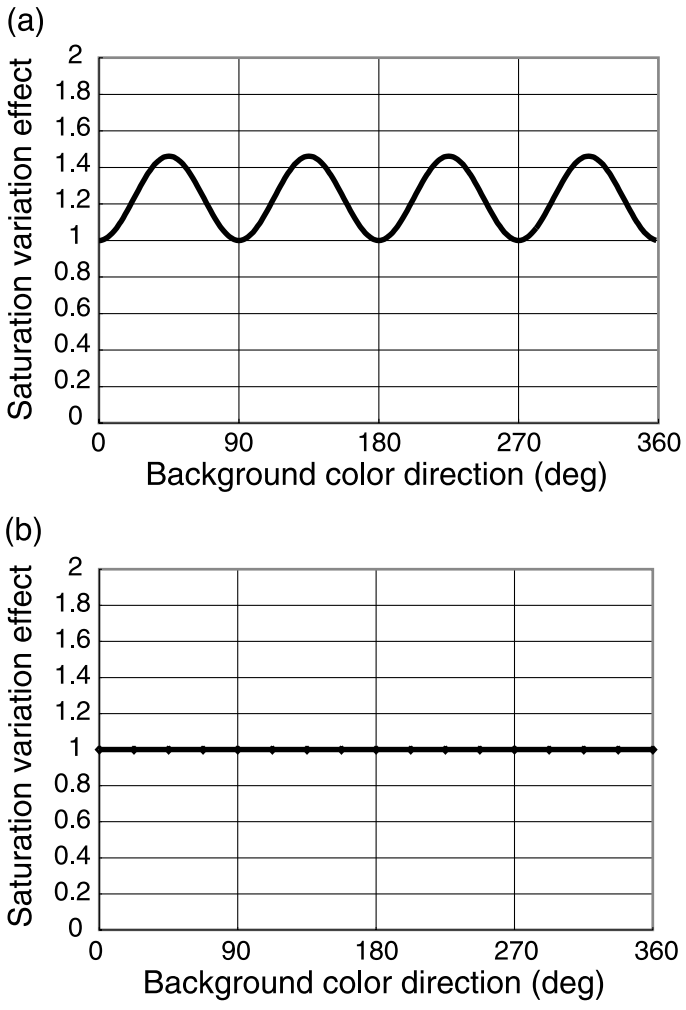

Figure 7. Expectations of effects of the saturation variation on shape discrimination thresholds in the cases (a) that only the cone-opponent channels are responsible for shape discrimination performance, and (b) that only mechanisms that completely distinguish between hue and saturation were responsible for task performance. Value 1 of the ordinate means that there is no effect, and values more than 1 means that saturation variation raises thresholds.

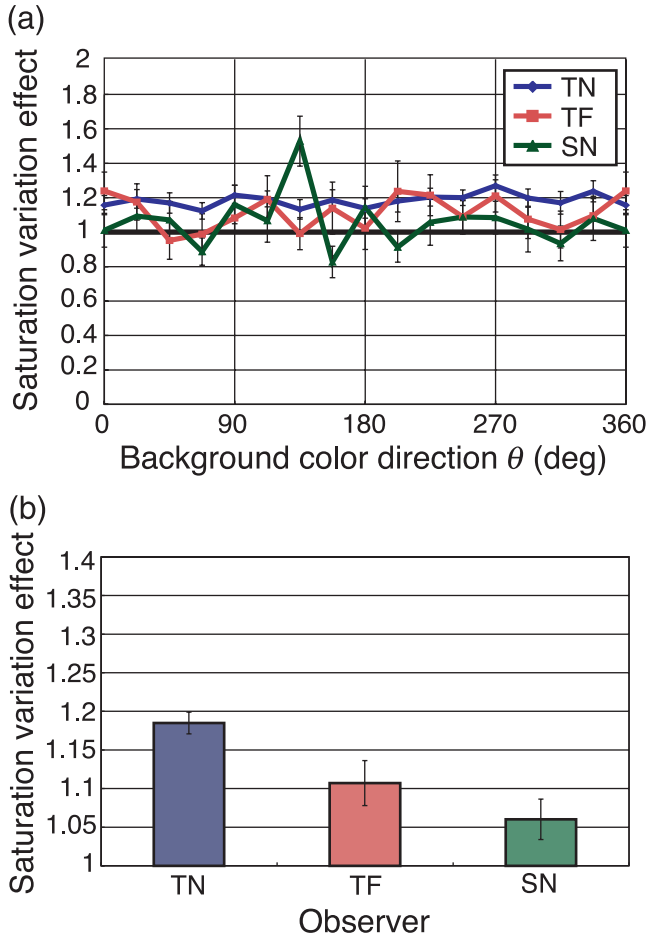

Figure 8. Saturation Variation Effects (SVEs) of Experiment 1. (a) SVEs as functions of the background color direction. (b) SVEs averaged across the background color directions. Error bars represent the standard errors derived from the Delta method (Oehlert, 1992).

based on color direction differences. But the main effects of the background color direction were not statistically significant for all observers; the magnitude of the saturation variation effect was nearly uniform across the color directions. The SVEs averaged across the background color directions are shown in Figure 8b. The SVEs were significantly more than 1 for all observers (the significance level was set at $\alpha = 0.05$), again indicating the effectiveness of saturation variation as a noise source.

Discussion

The saturation variation increased shape discrimination thresholds equally for all color directions. These effects are different from both of the expectations shown in Figures 7a and 7b, suggesting that the cone-opponent channels are not responsible for determining shape discrimination thresholds, and that mechanisms that do not completely distinguish between saturation and hue information are involved in shape discrimination. The effects of saturation on the thresholds within single saturation conditions (Figure 6) also support the idea that hue and saturation are not independently processed in conducting the shape discrimination task. One such scheme postulates multiple channels tuned to different hues, as suggested by several recent studies (e.g., Goda & Fujii, 2001; Kuriki, 2007; Li & Lennie, 1997).

The SVE values themselves are not so important, because they should vary with different factors in averaging the thresholds for the single-saturation condition: for example, number of saturations, range of saturations, and calculation methods for averaging. However, SVEs should be more than 1 respective of these factors. For example, averaging the results for the single-saturation condition in sensitivity (reciprocal of the thresholds) not in the thresholds raises SVEs due to decrease in the averaged threshold. Averaging the thresholds using more saturation levels for the single-saturation condition also raises SVEs. Therefore, the suggestion that hue and saturation are not independently processed should not be drawn only from the SVE calculation method employed here.

The effects of saturation variation were not very strong. One of the possible reasons for the weakness of the effects is that the range of the saturation variation was narrow. Saturation variations over a larger range might yield stronger noise effects. However, some investigations of the effect of noise on color discrimination (Gegenfurtner & Kiper, 1992; Li & Lennie, 1997) reported that the noise effect is quite weak when the signal and noise directions in a color space were orthogonal. Therefore noise effects of saturation variation on performance of tasks relying on hue differences might be intrinsically weak, since they are orthogonal. This explanation assumes an organization of the multiple-chromatic-channels type discussed above.

Though the shape discrimination thresholds varied with the background color direction, the shapes of the color direction-threshold functions were different across observers. As will be shown in the results of Experiment 2, thresholds for the region detection task also change with the background color direction, and these change tendencies also exhibit individual differences. Therefore, we cannot consider the individual differences of function-shapes in Figure 2 as individual differences of chromatic properties of mechanisms underlying shape discrimination. We will discuss the shapes of the color direction-threshold functions in the "Comparison between shape discrimination and region detection" section below.

We used five shapes of the test region determined in advance; results for different shape combinations might differ because similarities of shapes and spatial frequency components depend on the shape combinations. To check this point, observer TN replicated 5 sessions for the multiple-saturation condition of Experiment 1, and the results were separately analyzed in each shape

combination. There was no significant difference in color direction-threshold functions between different shape combinations.

Experiment 2—Region detection

Methods

Stimulus

We used the same apparatus in Experiment 2 as in Experiment 1. The stimulus was quite similar to that used in Experiment 1. The number of elements, the shapes of elements, texture size, and color distributions of the test and background regions were all the same as Experiment 1. The only difference in the stimulus from Experiment 1 was the number and shape of the test region. In Experiment 2, the stimulus had only one test region at the center of 4 white dots in Figure 1a at either left or right randomly. The test region was a 4.25 deg × 4.25 deg square, and was not rotated like Experiment 1 (that is, it was always upright).

Procedure

The procedure was also similar to Experiment 1 except for the observer's task. The two stimuli were successively presented for 247 ms each and interleaved by a gray background presentation for 1000 ms. Unlike Experiment 1, one stimulus had no test region, and the other had a test region. The observer indicated which stimulus had a test region according to the 2AFC procedure after the stimulus presentation. The other procedures, the method of threshold estimation, and the observers were the same as in Experiment 1.

Results

Thresholds

The thresholds measured in Experiment 2 are shown in Figure 9, and they are also shown in Figure 10 in the form of polar plots. The thresholds significantly varied with the background color direction ($p < 0.001$ for all observers) and decreased as the saturation increased ($p < 0.001$ for all observers) like the results of Experiment 1. The thresholds for the multiple-saturation condition (where saturation ranged from 15 to 30) exceeded even those for the single-saturation condition whose saturation was 15 in some cases, suggesting that the saturation variation acted as noise that limits simple region detection performance as well as shape discrimination performance. The thresholds averaged across the background color directions are shown in Figure 11. The results were quite similar to those in the shape discrimination task; the thresholds in the color direction difference increase with saturation, the threshold for the multiple-saturation condition seems high in comparison with the overall threshold levels for the single-saturation condition, and the thresholds in the Euclidian distance are also not independent of the saturation.

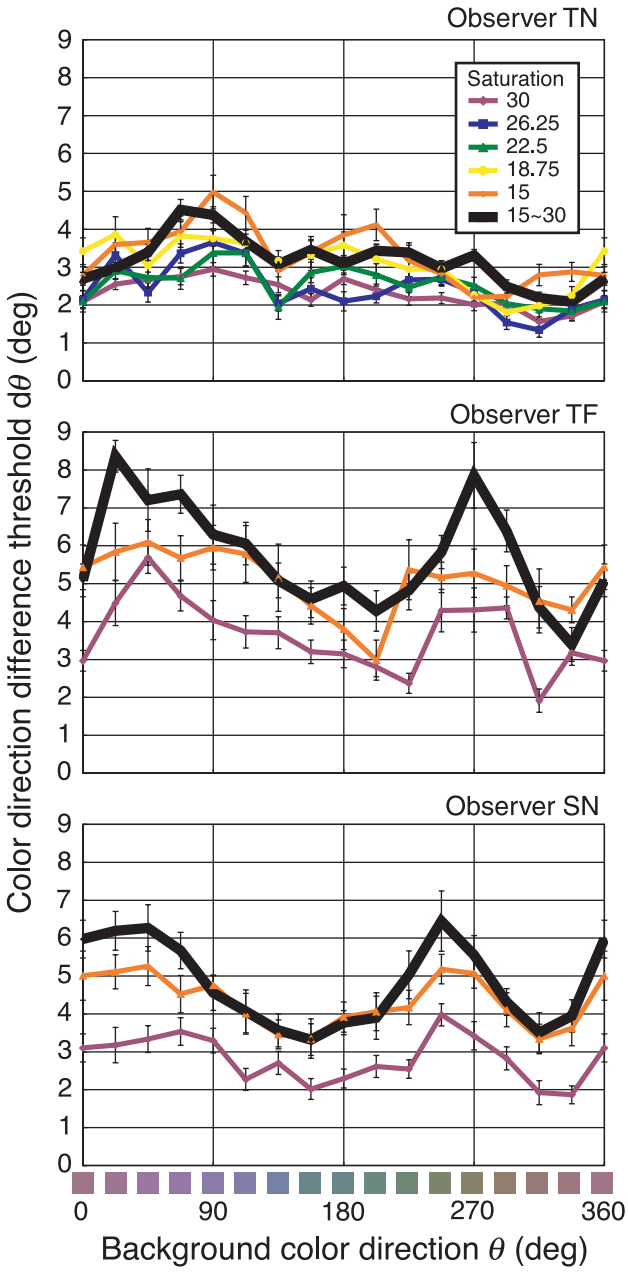

Figure 9. Region detection thresholds measured in Experiment 2. Expressions are the same as Figure 4.

The shapes of color direction-threshold functions seemed similar within each observer, but different across observers as in Experiment 1. Moreover interestingly, the shapes of the functions seemed different between Experiments 1 and 2 even within each observer. For observer TN, for example, the functions of Experiment 1 had a peak around the background color direction of 90 deg, while those of Experiment 2 had two peaks around color directions 90 deg and 180 deg. We compare these functions more precisely in the next section.

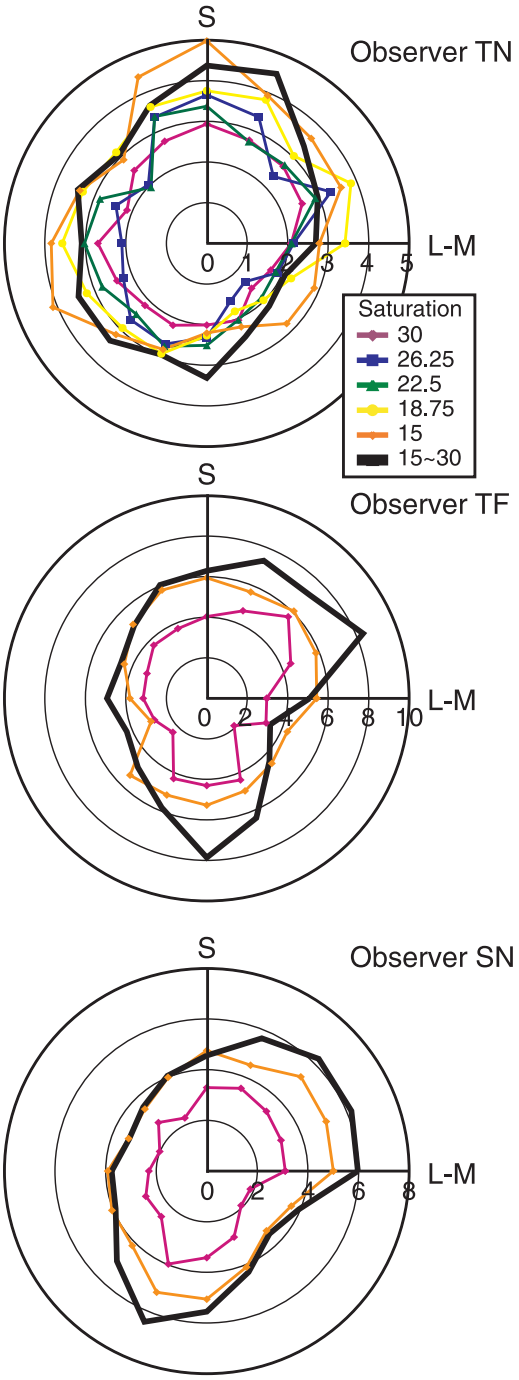

Figure 10. Region detection thresholds shown in the form of polar plots. Expressions are the same as Figure 5.

Effects of saturation variation

The SVEs, the effects of saturation distribution, calculated in the same way as Experiment 1 as functions of the background color direction are shown in Figure 12a. The SVEs for all observers were more than 1 in almost all color directions. The main effects of the background color direction were not statistically significant for two observers TF and SN (but $p < 0.01$ for TN). The function shapes in Figure 12a were again different from the expectations in

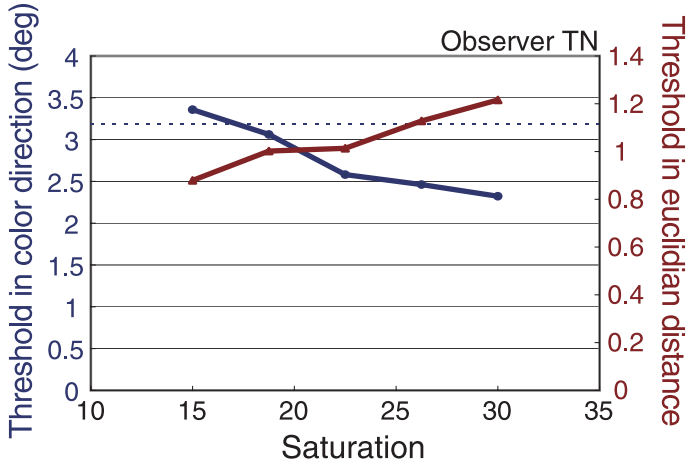

Figure 11. Region detection thresholds for the single-saturation condition averaged across the background color directions as functions of the stimulus saturation. Expressions are the same as Figure 6.

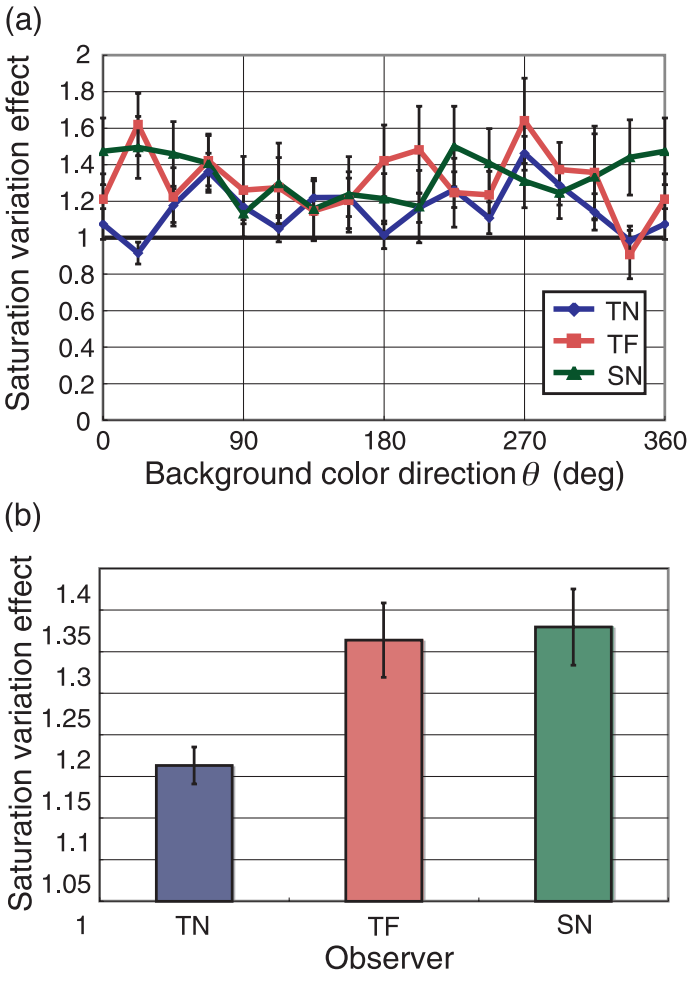

Figure 12. Saturation Variation Effects (SVEs) of Experiment 2. (a) SVEs as functions of the background color direction. (b) SVEs averaged across the background color directions. Error bars represent the standard errors derived from the Delta method (Oehlert, 1992).

Figures 7a and 7b. Figure 12b shows the SVEs averaged across the background color directions. The SVEs for all observers were significantly more than 1 (the significance level was set at $\alpha = 0.05$), indicating that the saturation variations increased the region detection thresholds.

Discussion

For two observers TF and SN, the saturation variations increased thresholds to a similar degree for all color directions. For the observer TN, the main effect of the background color direction was significant but did not take the form of the peaks at the cardinal directions shown in Figure 7a. Consequently, the SVEs for all observers were different from the expectations in both Figures 7a and 7b, suggesting that the region detection does not rely only on responses of the cone-opponent channels, and is not based only on mechanisms that completely distinguish between hue and saturation.

The shapes of color direction-threshold functions were different between Experiments 1 and 2 for each observer (as discussed further below), though the region detection thresholds also changed with the background color direction. These differences may reflect differences in chromatic information coding of mechanisms involved in those two tasks.

Comparison between shape discrimination and region detection

Differences in shapes of threshold functions

To compare the shapes of the color direction-threshold functions between the shape discrimination and region detection tasks, we divided the shape discrimination thresholds by the region detection thresholds for each observer and condition. The results for observer TN are shown in Figure 13a. The threshold ratios significantly varied with the background color direction ($p < 0.001$), while the interaction between the saturation condition and the background color direction was not statistically significant ($p > 0.1$). Threshold ratios averaged across the saturation conditions for all observers are shown in Figure 13b. Again, all observers' ratios changed with the background color direction ($p < 0.001$ for all observers), indicating that the shapes of color direction-threshold functions were different between the two tasks. Moreover, the shapes of the functions were similar for all saturation conditions (Figure 13a) and all observers (Figure 13b); they tended to have peaks around 135 deg and 315 deg. Thus the individual differences of the function shapes seen in Figures 4 and 9 disappeared by calculating the threshold ratios, indicating that the differences in the function shapes between the two tasks were similar across the observers in spite of the individual differences in the function shapes observed in the results of each task.

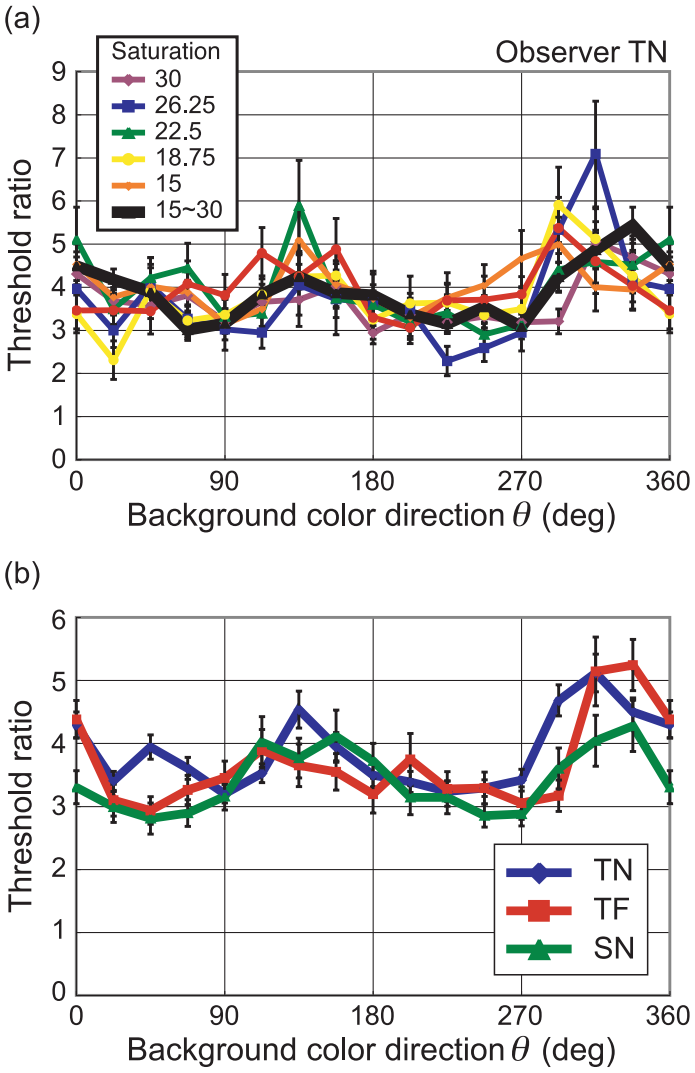

Figure 13. Shape discrimination thresholds divided by region detection thresholds (a) for all saturation conditions for observer TN, and (b) averaged over saturation conditions for all observers. The line colors represent different saturation conditions in (a), and different observers in (b).

Experiments 3 and 4: Effects of spatial frequency and orientation extraction

One of the important issues about the difference in results of the shape discrimination and region detection tasks is what difference between those tasks yielded the difference in chromatic properties of thresholds; plausible candidates include, for example, necessary spatial frequency components, a requirement for local orientation extractions, and integration of those local orientations.

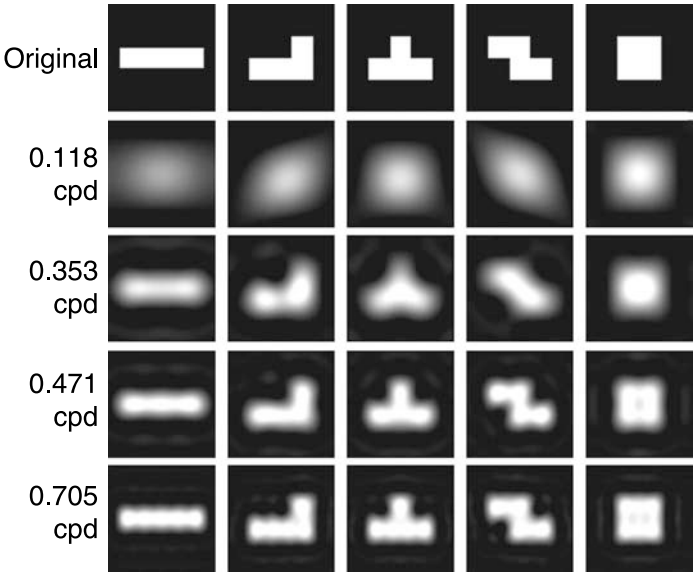

Figure 14. Shapes of the test region whose spatial frequency components higher than the left values are removed.

The chromatic channels of our visual system show low-pass spatial frequency properties (Kelly, 1983; Mullen, 1985). Because the shape discrimination task should require higher frequency components than the region detection task, the shape discrimination thresholds should be higher than region detection thresholds, and this is consistent with our results. In order to consider the effects of spatial frequency on the thresholds, we checked how high spatial frequency components are required to perform our shape discrimination task. Figure 14 shows the images of test shapes in which spatial frequency components higher than that shown in the left column were removed. These images suggest that spatial frequency components up to at least about 0.35 cpd might be required for our shape discrimination task, while the region detection task should require only much lower frequency components. Additionally, we confirmed that spatial frequency components higher than at least 0.47 cpd rarely affected shape discrimination thresholds in a further experiment, in which the observer performed the shape discrimination task using test regions without spatial frequency components higher than 0.47 cpd. In the results of Mullen (1985), chromatic sensitivity seems invariant for the spatial frequencies under 0.35 cpd, and sensitivities on the L-M and S axes do not seem so different, suggesting the possibility that differences in spatial frequency components necessary for the two tasks cannot explain the differences in chromatic properties of our thresholds. However, Mullen did not investigate contrast sensitivity functions for different color directions as in our experiments. Meanwhile, some previous studies (Beaudot & Mullen, 2005; Webster & De Valois, 1990) examined the properties of chromatic orientation channels, such as orientation discrimination thresholds and orientation tuning widths. They suggested that there is little difference in those properties between the L-M and S axes, though they also did not use stimuli with different color directions.

In Experiments 3 and 4, we examined the possibility that those two factors, spatial frequency and orientation extraction, could affect shapes of color direction-threshold functions using a texture stimulus similar to those in Experiments 1 and 2 but with chromatic Gabor patches instead of the test regions (Figure 15). The texture was composed of square elements with no gap between them, unlike the textures used in Experiments 1 and 2.

In Experiment 3, we examined the effects of spatial frequency on chromatic properties of thresholds. The stimulus is shown in Figure 15a. The Gabor patch had a color direction modulation whose saturation was 22.5 in the isoluminant plane without relation to the square shapes of small elements constituting the texture. Its spatial

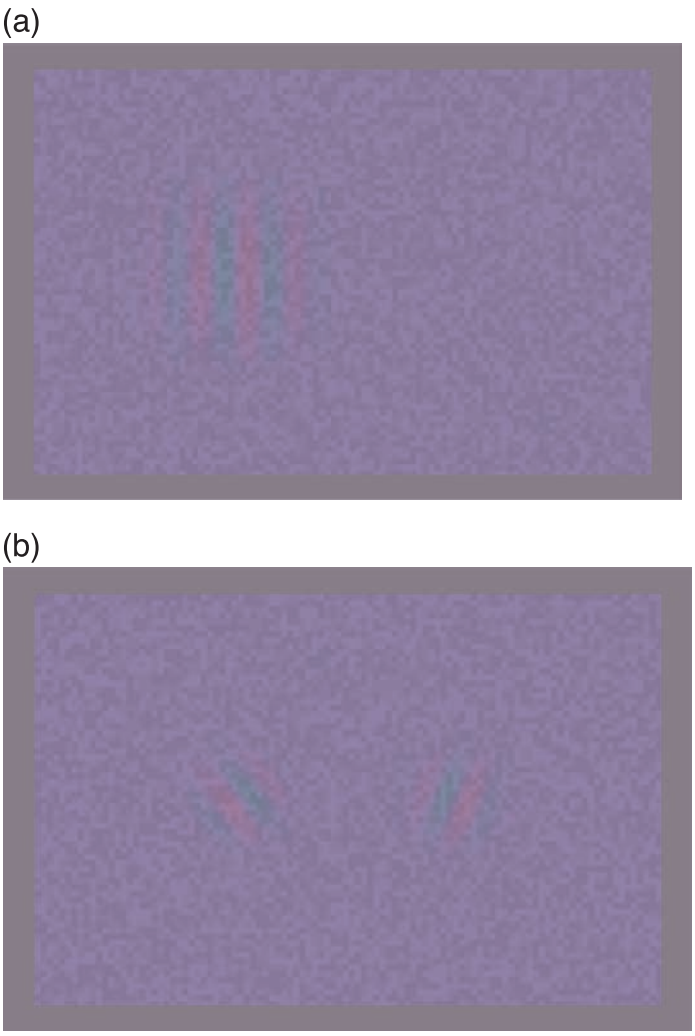

Figure 15. (a) Stimulus used in Experiment 3 to examine effects of spatial frequency. (b) Stimulus used in Experiment 4 to examine effects of necessity for orientation extraction.

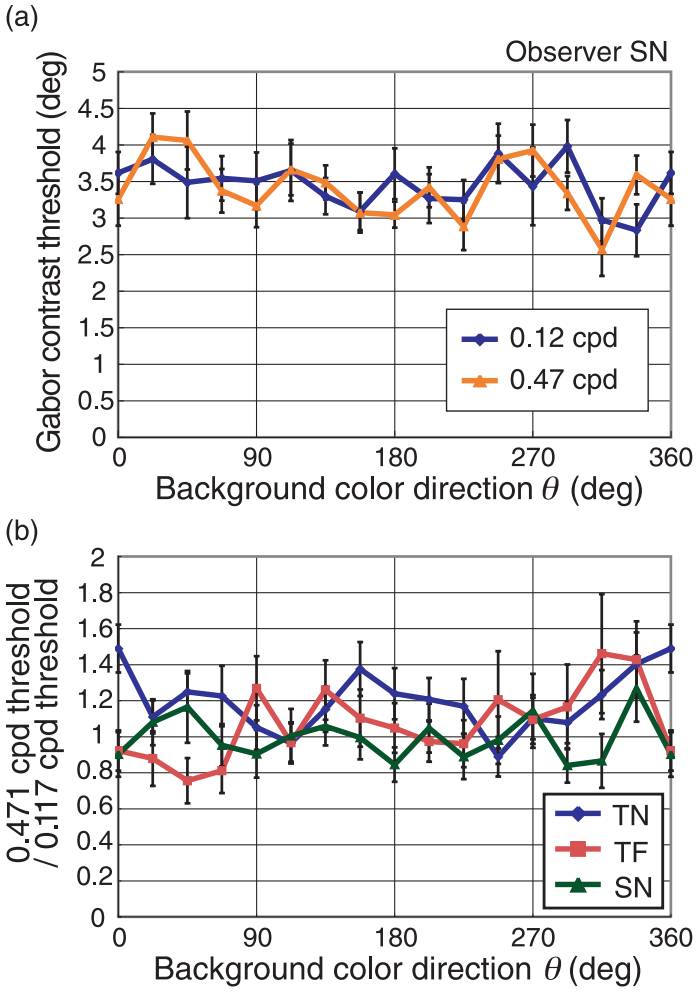

Figure 16. (a) Detection thresholds of Gabor contrast for observer SN. The colors of plots represent different spatial frequencies of Gabor patches. (b) Thresholds for 0.47 cpd divided by those for 0.12 cpd.

frequency was either 0.12 or 0.47 cpd. The elements were used only to create random luminance modulations ranging from −7.5 to 7.5 threshold units. Thus chromaticity varied in accordance with Gabor patch and luminance randomly varied with small elements in the stimulus. The experimental procedure was quite similar to that of Experiment 2, except that one of two stimuli presented successively had a Gabor patch instead of a test region. We measured detection thresholds in terms of Gabor contrast: the threshold angular difference in color space between test and background necessary for detection of the Gabor patches. These thresholds are shown in Figure 16a. The shapes of threshold functions for two different frequencies were similar. The ratios of thresholds for 0.47 cpd to those for 0.12 cpd are shown in Figure 16b. In this result, the main effect of the background color direction was not statistically significant for any observers, and the variations were not consistent across observers. These results suggest that at least in the range of spatial frequency our shape discrimination and region detection tasks require, spatial frequency does not affect threshold function shapes, that is, the differences in spatial frequency components required by those two tasks cannot explain the differences in threshold function shapes between those tasks.

In Experiment 4, we examined whether the requirement for orientation extraction could affect shapes of threshold functions. The stimulus was similar to that of Experiment 3 except that it has two Gabor patches whose spatial frequencies were 0.47 and whose orientations were random but always different from each other by 30 deg. The observer judged whether the orientations of the two Gabor patches were different or not. Thresholds of Gabor contrasts for orientation discrimination were measured. The measured thresholds are shown in Figure 17a with the detection thresholds measured in Experiment 3. Even

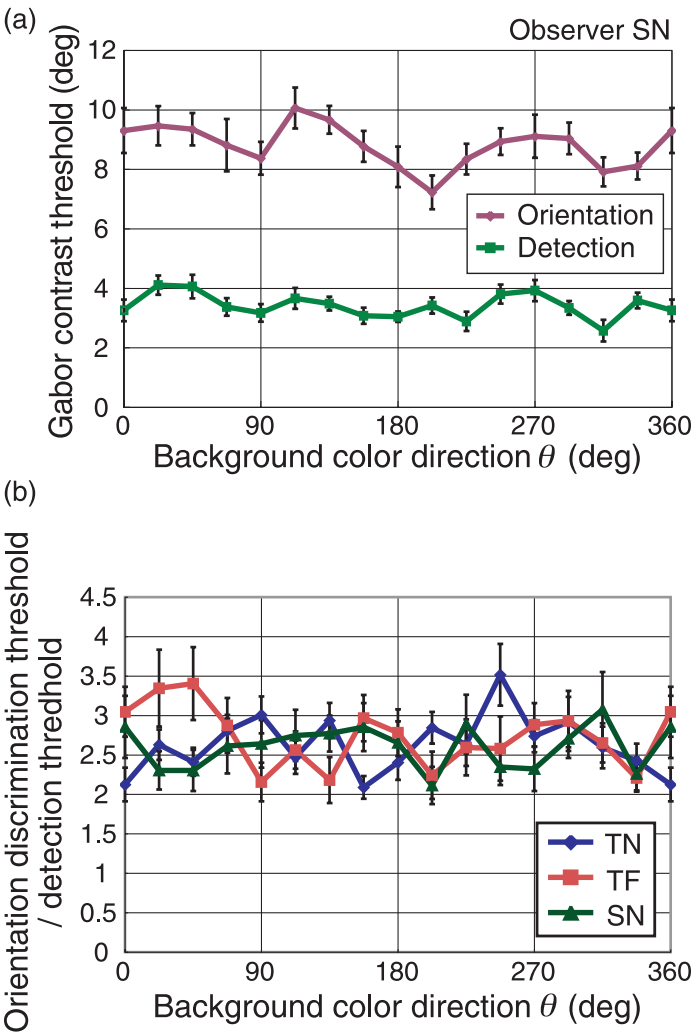

Figure 17. (a) Orientation discrimination thresholds of Gabor contrast for observer SN as compared with detection thresholds. The purple plots represent the orientation discrimination thresholds, and the green ones represent the detection thresholds. (b) Orientation discrimination thresholds divided by detection thresholds.

though the general magnitude of thresholds for mere detection and orientation discrimination was different, those shapes look similar. The ratios of orientation discrimination thresholds to detection thresholds are shown in Figure 17b. As in Figure 16b, the main effects of the background color direction were not significant for all observers, suggesting the requirement for orientation extraction has little effect on the chromatic properties of thresholds, and therefore cannot explain the difference in shapes of the threshold functions between our shape discrimination and region detection tasks. In addition, the similarity of function shapes—despite the differences in general threshold magnitudes between the detection and orientation discrimination tasks—suggests that nonlinearity of hue coding may also not be a cause of the difference in threshold functions between our shape discrimination and region detection tasks.

Though we could not find any effects of spatial frequency and orientation extraction from Experiments 3 and 4, there is a possibility that this is because the effect of each of those factors was too weak to be found in the results. In that case, the summed effects of those two factors might yield a difference in threshold function shapes. To check this, we compared the detection thresholds for 0.12 cpd and orientation discrimination thresholds for 0.47 cpd. In the results (not shown), the function shapes were again not significantly different between those thresholds.

General discussion

Effects of saturation variation

Saturation variation increased both the shape discrimination thresholds and the region detection thresholds. In addition, the effects were not so different between background color directions, and at least the magnitudes of the effects did not increase at the cardinal directions. These results suggest that the thresholds for both tasks are determined neither by responses of the cone-opponent channels, nor by mechanisms that completely distinguish between hue and saturation.

Several previous studies have demonstrated that color discrimination thresholds from suprathreshold reference colors cannot be accounted for only by responses of the cone-opponent channels (Krauskopf & Gegenfurtner, 1992; Sankeralli & Mullen, 1999). In addition, several previous studies examining color discrimination by means of noise masking techniques have suggested that the cone-opponent channels are not enough to explain the results of color discrimination experiments (D'Zmura & Knoblauch, 1998; Gegenfurtner & Kiper, 1992; Goda & Fujii, 2001; Hansen & Gegenfurtner, 2006; Li & Lennie, 1997; Lindsey & Brown, 2004), though some studies do not support this idea (Eskew, Newton, & Giulianini, 2001; Giulianini & Eskew, 1998; Sankeralli & Mullen, 1997). In view of the present finding that the thresholds were not determined only by mechanisms that completely distinguish between hue and saturation, the shape discrimination and region detection tasks may rely on responses of multiple channels tuned to different hues as suggested by those previous studies.

Sankeralli and Mullen (1999) investigated the separation of hue and saturation in visual processing. They presented the observer with two lights successively whose hues were different, and measured the hue discrimination thresholds. The results showed that the thresholds were determined by the color direction difference on the isoluminant plane, and that, more importantly, temporal variation of saturation rarely affected the thresholds. They concluded that hue and saturation information are separately processed even in relatively early visual processing. On the other hand, our results on region detection (Experiment 2) showed that saturation variation acted as noise in raising hue difference thresholds. One difference between their experiments and ours is that in our displays the stimuli to be discriminated were separated spatially rather than temporally. Because our task was to discriminate two regions spatially adjacent to each other, the effects of rather lower level mechanisms such as the double-opponent receptive field (Conway, 2001; Lennie, Krauskopf, & Sclar, 1990) might be involved in the results. On the other hand, as the two stimuli of Sankeralli and Mullen's experiments were temporally separated, some higher-order mechanisms such as short-term memory might have an important role in performing their task. Therefore their results suggesting separation of hue and saturation may be valid only in specific situations.

Individual differences in threshold function shapes

The thresholds for both the shape discrimination and region detection tasks varied with the background color direction. However, the shapes of color direction-threshold functions for each task were different between observers. Possible causes of these individual differences may be, for example, adjustment of saturation based on the differences in the thresholds measured in the preliminary experiment between + and − directions (from a to a'), normalization of the axes of the DKL space based on each observer's discrimination thresholds, and individual differences in the direction of the cardinal axes (Webster, Miyahara, Malkocv, & Raker, 2000), since these factors could change the distance in color space corresponding to a certain color direction difference. For example, Webster et al. (2000) reported that the direction of the S axis averaged across the six observers was 99.6 deg, 10 deg different from that of the standard observer (90 deg). In this case, the distance in the individual space correspond-

ing to a certain color direction difference at color directions around 45 and 225 deg in the standard observer's space should decrease. This might lead to larger thresholds of color direction at background color directions around 45 and 225 deg.

Therefore, we examined the possibility that the factors described above could affect the shape discrimination and region detection thresholds, assuming that the color direction difference threshold was determined as a certain distance in color space for each saturation condition. First, in order to examine the effects of saturation adjustment based on the preliminary threshold differences in + and − directions, we calculated the distances in the no-saturation-adjusted color space (where saturation is defined with a) corresponding to color direction differences of 1 deg in the saturation-adjusted color space (where saturation is defined with a'). The thresholds measured in our experiments should be inversely proportional to those distances if the thresholds were determined based on distances in the color space. The thresholds averaged across saturation conditions and the reciprocals of the calculated distances for observer TN are shown in Figure 18. The thresholds and reciprocal distances are normalized by their own means across the background color directions. They appeared to be similar to some extent, and this tendency was the same for the other observers. This suggests that the saturation adjustment can be one of the possible causes of the individual differences in threshold variations with the background color direction; at least in our stimulus and color conditions our saturation adjustment based on each of thresholds for + and − directions on each axis may not have worked well.

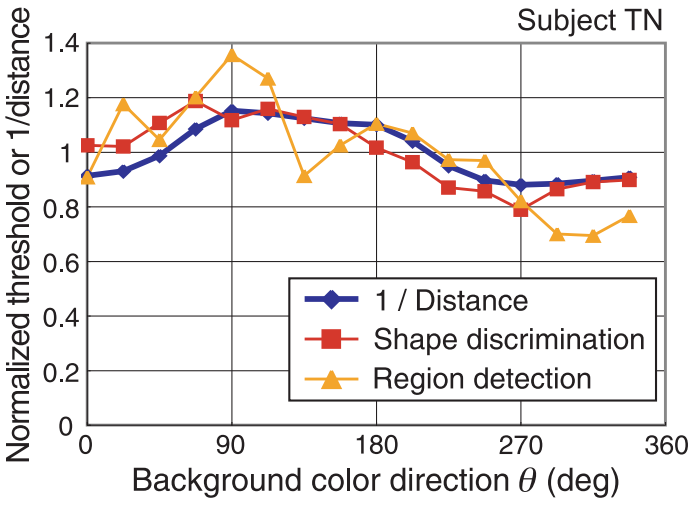

Figure 18. Thresholds of Experiments 1 and 2 averaged between saturation conditions, and reciprocals of distances in the no-saturation-adjusted color space (where saturation is defined with a) corresponding to color direction differences of 1 deg in the saturation-adjusted color space (where saturation is defined with a'). They are normalized by their own means across the background color directions.

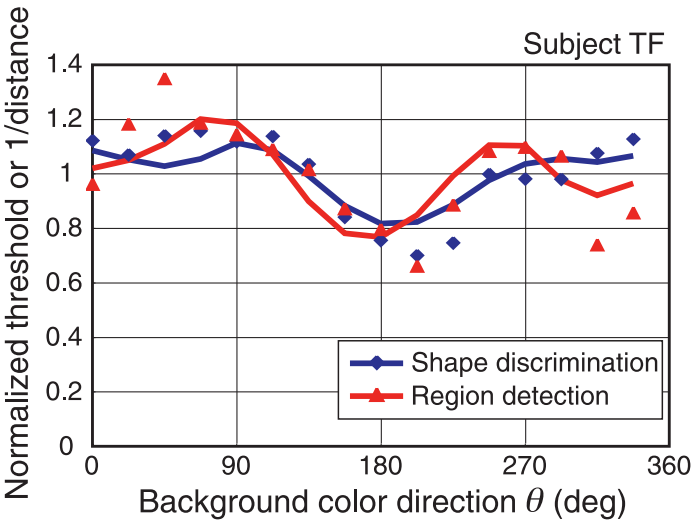

Figure 19. Normalized thresholds and reciprocals of distances in the space adjusted by the two parameters (see text) corresponding to a color direction difference of 1 deg in the non-adjusted space. The plots are the thresholds, and the lines are the reciprocals of distances.

However, some differences still appeared between the shapes of the reciprocal distance and thresholds in Figure 18. And of course, the reciprocal distance cannot explain the difference in shapes of threshold functions between the shape discrimination and region detection tasks, discussed below.

Next, we introduced two free parameters (in addition to just removing the effect of the saturation adjustment) in an attempt to further improve the account of the shapes of threshold functions. One of them is the relative scaling of the L-M and S axes, which could test the efficiency of normalization of each axis. The other is an ad hoc adjustment in the direction of the S axis as suggested by Webster et al. (2000). These two free parameters were adjusted so that square errors between the reciprocal distances and the normalized thresholds were minimized. The reciprocal distances and the thresholds for observer TF are shown in Figure 19. The reciprocal distances traced the thresholds reasonably well, suggesting that adjustment of the space using these two parameters helps explain threshold variations. This tendency was similar for the other observers. Figure 20 shows the best-fitting parameter values for the shape discrimination and region detection tasks. The values were different across observers and tasks, suggesting that these factors may be largely responsible for the individual differences in threshold variations.

Differences of shape discrimination and region detection

Although the shapes of the color direction-threshold functions had individual differences for each of the shape

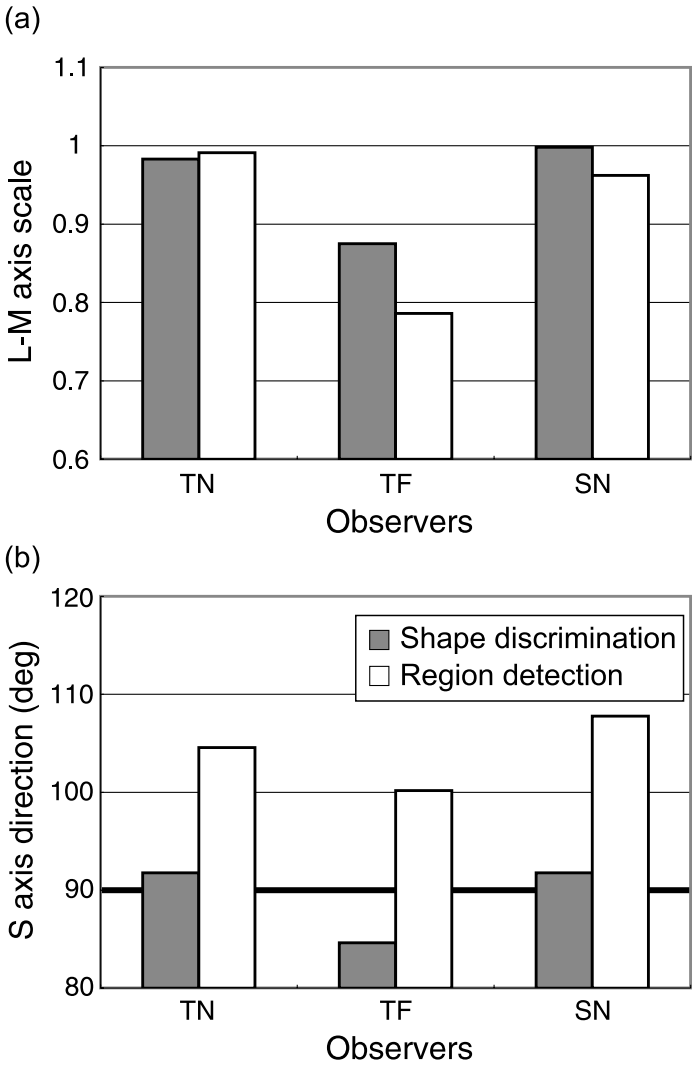

Figure 20. Two adjusted parameters. (a) Relative scaling of the normalized L-M axis to the normalized S axis (i.e., value 1 means that the normalization of these axes with the preliminary thresholds worked well in terms of correspondence between the thresholds and reciprocal distances). (b) Direction of the S axis.

discrimination and region detection tasks (Figures 4 and 7), the threshold ratios between the two tasks showed a pattern of variation that is consistent across observers (Figure 13). Because the effects of the individual factors such as directions of the cardinal axes should be diminished in calculating the threshold ratios, this consistency indicates that there are genuine differences between the chromatic coding of information for the two tasks.

What differences in chromatic coding could cause the differences in threshold function shapes? If shape discrimination and region detection relied on the responses of multiple channels as suggested by the effects of saturation variation, differences in the number of channels and their preferred hue could be possible causes for differences in chromatic properties, though we did not investigate those properties. In addition, the adjusted directions of S axes were tilted more clockwise for shape discrimination than for region detection for all observers, as shown in Figure 20; the average direction of the S axis for region detection was 104.2 deg, closer to the report by Webster et al. (2000), while for shape discrimination, it was 89.4 deg. Perhaps, then, the effective directions of the cardinal axis were different for the two tasks. This effect of the cardinal directions can also be intuitively expected from our results. Figure 21a shows a polar plot of Figure 13b. This plot looks like an ellipse, and this elliptical shape can be easily created just by changing the direction of the cardinal axis. For example, in Figure 21b, a color circle in a cone-opponent space becomes an ellipse in another space whose direction of the S axis is slightly different. However, our results did not show at what level of chromatic processing these apparent differences of chromatic properties occur. To investigate causes of these differences in threshold function shapes, more experi-

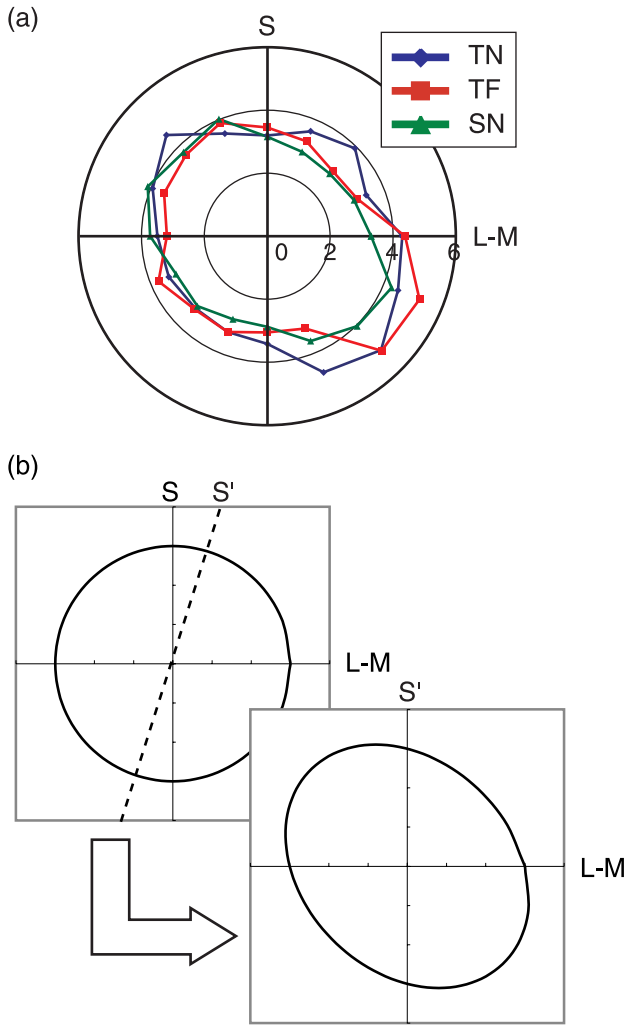

Figure 21. (a) Polar plot of Figure 13b. (b) Color circle in a cone-opponent space. It becomes an ellipse in another space whose cardinal axis direction is different.

ments using other techniques such as noise masking (Hansen & Gegenfurtner, 2006) would be necessary.

What differences between the shape discrimination task and the region detection task yielded these differences in threshold function shapes? In many models of form processing in the human visual system (Wilkinson et al., 1998; Wilson & Wilkinson, 1998), local orientations are analyzed at the first stage, and then the local orientations are globally integrated to construct the entire shape of an object. The results of Experiments 3 and 4 confirmed that differences in spatial frequency under 0.47 cpd and the requirement for orientation extraction have little or no effect on the threshold function shapes. Accordingly, the chromatic properties of the mechanisms underlying chromatic detection are likely to be similar to those underlying local orientation extraction in form processing. The difference in threshold function shapes between shape discrimination and region detection may instead reflect differences in chromatic coding between mechanisms for chromatic discrimination (or simple orientation extraction) and global spatial integration of border properties for form perception. Previous experiments using chromatic Glass patterns (Cardinal & Kiper, 2003; Mandelli & Kiper, 2005) suggested that the chromatic tuning widths differ between the first stage and the second stage of form processing. Although our results cannot be directly compared with their results, they are in agreement with the idea that chromatic properties are different between stages of form processing.

Some physiological and brain imaging studies have suggested that local orientations are extracted in V1 (Smith, Bair, & Movshon, 2002), and global form information such as linkage of contour and global shape of a Glass pattern is processed in V4 (Gallant, Braun, & Vanessen, 1993). Our results do not clarify precisely the characteristics of chromatic mechanisms such as the tuning width or the numbers of chromatic channels underlying these two stages of form processing, but suggest only that hue coding may be different between the stages. However, our results may be helpful for characterizing the stream of chromatic information processing in the brain, especially from V1 to V4, by suggesting that preferred hue ranges are different between those two stages.

Conclusions

We measured thresholds of the color direction differences required for two different tasks: shape discrimination and region detection. First, thresholds for both tasks increased equally across color directions when saturation variation was added to the stimulus, suggesting that these tasks do not rely solely on the responses of the cone-opponent channels, or on mechanisms that completely distinguish between hue and saturation information. Second, the shapes of color direction-threshold functions were different between the two tasks, and the differences were uniform across observers. These results suggest that hue coding is different for shape discrimination and region detection. This difference could reflect the rotation of the direction of the S axis. Finally, Experiments 3 and 4 confirmed that the two factors, spatial frequency and requirement for orientation extraction, did not affect the shapes of color direction-threshold functions in our two tasks. Considering that forms are separately processed in at least two stages, these results suggest the possibility that chromatic properties for shape discrimination different from those for region detection arise at the second stage of form processing where local orientations are globally integrated.

Acknowledgments

We thank Hirohiko Kaneko, Ichiro Kuriki, and Shin'ya Nishida for their valuable discussions, Donald MacLeod for his help and comments, Tiffany Ho for revising the English expressions in this manuscript, and two reviewers for their valuable comments and suggestions to improve this manuscript. Preparation of the manuscript was supported by NIH EY01711.

Commercial relationships: none.
Corresponding author: Takehiro Nagai.
Email: nagai@bpel.ics.tut.ac.jp.
Address: Department of Information and Computer Sciences, Toyohashi University of Technology, 1-1 Hibarigaoka Tenpaku, Toyohashi 441-8580, Japan.

References

Beaudot, W. H. A., & Mullen, K. T. (2005). Orientation selectivity in luminance and color vision assessed using 2-d band-pass filtered spatial noise. *Vision Research, 45,* 687–696. [PubMed]

Boynton, R. M. (1979). *Human color vision*. New York: Holt, Rinehart and Winston, 1979.

Boynton, R. M., & Kambe, N. (1980). Chromatic difference steps of moderate size measured along theoretically critical axes. *Color Research and Application, 5,* 13–23.

Boynton, R. M., Nagy, A. L., & Olson, C. X. (1983). A flaw in equations for predicting chromatic differences. *Color Research and Application, 8,* 69–74.

Cardinal, K. S., & Kiper, D. C. (2003). The detection of colored Glass patterns. *Journal of Vision, 3*(3):2, 199–208, http://journalofvision.org/3/3/2/, doi:10.1167/3.3.2. [PubMed] [Article]

Conway, B. R. (2001). Spatial structure of cone inputs to color cells in alert macaque primary visual cortex (V-1). *Journal of Neuroscience, 21,* 2768–2783. [PubMed] [Article]

Derrington, A. M., Krauskopf, J., & Lennie, P. (1984). Chromatic mechanisms in lateral geniculate nucleus of macaque. *The Journal of Physiology, 357,* 241–265. [PubMed] [Article]

D'Zmura, M., & Knoblauch, K. (1998). Spectral bandwidths for the detection of color. *Vision Research, 38,* 3117–3128. [PubMed]

Eskew, R. T., Newton, J. R., & Giulianini, F. (2001). Chromatic detection and discrimination analyzed by a Bayesian classifier. *Vision Research, 41,* 893–909. [PubMed]

Gallant, J. L., Braun, J., & Vanessen, D. C. (1993). Selectivity for polar, hyperbolic, and Cartesian gratings in macaque visual-cortex. *Science, 259,* 100–103. [PubMed]

Gegenfurtner, K. R., & Kiper, D. C. (1992). Contrast detection in luminance and chromatic noise. *Journal of the Optical Society of America A, 9,* 1880–1888. [PubMed]

Giulianini, F., & Eskew, R. T. (1998). Chromatic masking in the (Delta L/L, Delta M/M) plane of cone-contrast space reveals only two detection mechanisms. *Vision Research, 38,* 3913–3926. [PubMed]

Goda, N., & Fujii, M. (2001). Sensitivity to modulation of color discrimination in multi-colored textures. *Vision Research, 41,* 2475–2485. [PubMed]

Hansen, T., & Gegenfurtner, K. R. (2006). Higher level chromatic mechanisms for image segmentation. *Journal of Vision, 6*(3):5, 239–259, http://journalofvision.org/6/3/5/, doi:10.1167/6.3.5. [PubMed] [Article]

Kelly, D. H. (1983). Spatiotemporal variation of chromatic and achromatic contrast thresholds. *Journal of the Optical Society of America, 73,* 742–750. [PubMed]

Krauskopf, J., & Gegenfurtner, K. (1992). Color discrimination and adaptation. *Vision Research, 32,* 2165–2175. [PubMed]

Krauskopf, J., Williams, D. R., & Heeley, D. W. (1982). Cardinal directions of color space. *Vision Research, 22,* 1123–1131. [PubMed]

Kuriki, I. (2007). Aftereffect of contrast adaptation to a chromatic notched-noise stimulus. *Journal of the Optical Society of America A, 24,* 1858–1872. [PubMed]

Lennie, P., Krauskopf, J., & Sclar, G. (1990). Chromatic mechanisms in striate cortex of macaque. *Journal of Neuroscience, 10,* 649–669. [PubMed] [Article]

Li, A., & Lennie, P. (1997). Mechanisms underlying segmentation of colored textures. *Vision Research, 37,* 83–97. [PubMed]

Lindsey, D. T., & Brown, A. M. (2004). Masking of grating detection in the isoluminant plane of DKL color space. *Visual Neuroscience, 21,* 269–273. [PubMed]

Livingstone, M., & Hubel, D. (1987). Psychophysical evidence for separate channels for the perception of form, color, movement, and depth. *Journal of Neuroscience, 7,* 3416–3468. [PubMed] [Article]

MacAdam, D. L. (1942). Visual sensitivities to color differences in daylight. *Journal of the Optical Society of America, 32,* 247–274.

MacLeod, D. I. A., & Boynton, R. M. (1979). Chromaticity diagram showing cone excitation by stimuli of equal luminance. *Journal of the Optical Society of America, 69,* 1183–1186. [PubMed]

Mandelli, M. F., & Kiper, D. C. (2005). The local and global processing of chromatic Glass patterns. *Journal of Vision, 5*(5):2, 405–416, http://journalofvision.org/5/5/2/, doi:10.1167/5.5.2. [PubMed] [Article]

Mollon, J. D. (1989). "Tho' she kneel'd in that place where the grew ı " The uses and origins of primate colour vision. *Journal of Experimental Biology, 146,* 21–38. [PubMed] [Article]

Mullen, K. T. (1985). The contrast sensitivity of human colour vision to red-green and blue-yellow chromatic gratings. *The Journal of Physiology, 359,* 381–400. [PubMed] [Article]

Mullen, K. T., & Beaudot, W. H. A. (2002). Comparison of color and luminance vision on a global shape discrimination task. *Vision Research, 42,* 565–575. [PubMed]

Mullen, K. T., Beaudot, W. H. A., & MacIlhagga, W. H. (2000). Contour integration in color vision: A common process for the blue-yellow, red-green and luminance mechanisms? *Vision Research, 40,* 639–655. [PubMed]

Nagai, T., & Uchikawa, K. (2008). Characteristics of grouping colors for figure segregation on a multicolored background. *Journal of the Optical Society of America A, 25,* 2618–2629. [PubMed]

Oehlert, G. W. (1992). A note on the delta method. *The American Statistician, 46,* 27–29.

Sankeralli, M. J., & Mullen, K. T. (1997). Postreceptoral chromatic detection mechanisms revealed by noise masking in three-dimensional cone contrast space. *Journal of the Optical Society of America A, 14,* 2633–2646. [PubMed]

Sankeralli, M. J., & Mullen, K. T. (1999). Ratio model for suprathreshold hue-increment detection. *Journal of*

the Optical Society of America A, 16, 2625–2637. [PubMed]

Smith, M. A., Bair, W., & Movshon, J. A. (2002). Signals in macaque striate cortical neurons that support the perception of Glass patterns. *Journal of Neuroscience, 22,* 8334–8345. [PubMed] [Article]

Smith, V. C., & Pokorny, J. (1975). Spectral sensitivity of the foveal cone photopigments between 400 and 500 nm. *Vision Research, 15,* 161–171. [PubMed]

Stabell, U., & Stabell, B. (1984). Color-vision mechanisms of the extrafoveal retina. *Vision Research, 24,* 1969–1975. [PubMed]

Webster, M. A., & De Valois, K. K. (1990). Orientation and spatial-frequency discrimination for luminance and chromatic gratings. *Journal of the Optical Society of America A, 7,* 1034–1049. [PubMed]

Webster, M. A., Miyahara, E., Malkocv, G., & Raker V. E. (2000). Variations in normal color vision: I. Cone-opponent axes. *Journal of the Optical Society of America A, 17,* 1535–1544. [PubMed]

Wilkinson, F., Wilson, H. R., & Habak, C. (1998). Detection and recognition of radial frequency patterns. *Vision Research, 38,* 3555–3568. [PubMed]

Wilson, H. R., & Wilkinson, F. (1998). Detection of global structure in Glass patterns: Implications for form vision. *Vision Research, 38,* 2933–2947. [PubMed]

Wilson, J. A., & Switkes, E. (2005). Integration of differing chromaticities in early and midlevel spatial vision. *Journal of the Optical Society of America A, 22,* 2169–2181. [PubMed]

Wright, W. D., & Pitt, F. H. G. (1934). Hue-discrimination in normal colour-vision. *Proceeding Physical Society, 46,* 459–473.